Microstructural brain changes track cognitive decline in mild cognitive impairment

Emilie T. Reas[a,b,*], Donald J. Hagler Jr[b,c], Nathan S. White[b,c], Joshua M. Kuperman[b,c], Hauke Bartsch[b], Christina E. Wierenga[d,e], Douglas Galasko[c], James B. Brewer[a,c], Anders M. Dale[a,b,c], Linda K. McEvoy[b,c,f]

[a] Department of Neurosciences, University of California, San Diego, La Jolla, CA, USA
[b] Center for Multimodal Imaging and Genetics, University of California, San Diego, La Jolla, CA, USA
[c] Department of Radiology, University of California, San Diego, La Jolla, CA, USA
[d] Department of Psychiatry, University of California, San Diego, La Jolla, CA, USA
[e] Department of Veterans Affairs, San Diego Healthcare system, La Jolla, CA, USA
[f] Department of Family Medicine and Public Health, University of California, San Diego, La Jolla, CA, USA

ARTICLE INFO

ABSTRACT

Improved characterization of the microstructural brain changes occurring in the early stages of Alzheimer's disease may permit more timely disease detection. This study examined how longitudinal change in brain microstructure relates to cognitive decline in aging and prodromal Alzheimer's disease. At baseline and two-year follow-up, 29 healthy controls and 21 individuals with mild cognitive impairment or mild Alzheimer's disease underwent neuropsychological evaluation and restriction spectrum imaging (RSI). Microstructural change in the hippocampus, entorhinal cortex, and white matter tracts previously shown to be vulnerable to Alzheimer's disease, was compared between healthy controls and impaired participants. Partial correlations and stepwise linear regressions examined whether baseline RSI metrics predicted subsequent cognitive decline, or change in RSI metrics correlated with cognitive change. In medial temporal gray and white matter, restricted isotropic diffusion and crossing fibers were lower, and free water diffusion was higher, in impaired participants. Restricted isotropic diffusion in the hippocampus declined more rapidly for cognitively impaired participants. Baseline hippocampal restricted isotropic diffusion predicted cognitive decline, and change in hippocampal and entorhinal restricted isotropic diffusion correlated with cognitive decline. Within controls, changes in white matter restricted oriented diffusion and crossing fibers correlated with memory decline. In contrast, there were no correlations between rates of cortical atrophy and cognitive decline in the full sample or within controls. Changes in medial temporal lobe microarchitecture were associated with cognitive decline in prodromal Alzheimer's disease, and these changes were distinct from microstructural changes in normal cognitive aging. RSI metrics of brain microstructure may hold value for predicting cognitive decline in aging and for monitoring the course of Alzheimer's disease.

1. Background

As the prevalence of Alzheimer's disease (AD) continues to rise, identifying the earliest neurobiological changes that precipitate cognitive decline is of accelerating importance. Cortical atrophy, particularly in the medial temporal lobe, is one of the strongest biomarkers of prodromal AD and predictors of disease progression from mild to advanced stages of dementia (Brueggen et al., 2015; Du et al., 2001;

Jack Jr. et al., 2000; McDonald et al., 2012; McEvoy et al., 2009). However, evidence from diffusion MRI, which estimates fine architectural features from the diffusion properties within tissue, suggests that white matter degeneration may precede gray matter atrophy in AD (Agosta et al., 2011; Amlien and Fjell, 2014; Fletcher et al., 2013; L. Zhuang et al., 2012). Both gray and white matter microstructure, measured with diffusion tensor imaging (DTI), track disease progression (Kitamura et al., 2013; Nowrangi et al., 2013), predict cognitive decline and clinical conversion (Douaud et al., 2013; Fletcher et al., 2013; Lancaster et al., 2016; Mielke et al., 2012; L. Zhuang et al., 2012), and correlate with neuropathological burden along the AD continuum (Kantarci et al., 2017).

Though DTI can capture voxel-level changes in diffusion properties over the disease course, it is insensitive to sub-voxel architectural nuances that more accurately estimate complex tissue organization. Advanced imaging methods that expand upon the basic diffusion tensor model are capable of probing diffusion parameters that more closely approximate finer cytoarchitectural features. Using these tools, improved characterization of gray and white matter microstructural markers of cognitive decline will help to clarify the degenerative cellular events underlying AD progression, enabling earlier disease detection and more effective disease monitoring.

Restriction spectrum imaging (RSI) is a multishell, multicompartment diffusion MRI technique that more comprehensively characterizes tissue microstructure than DTI by dissociating free water, restricted (presumably intracellular) and hindered (presumably extracellular) diffusion compartments (White et al., 2013). Also in contrast to DTI, RSI estimates the contribution of crossing fibers (CF) and measures oriented and isotropic diffusion within a given voxel. In a recent cross-sectional analysis of RSI metrics, we reported declines in a combined measure of restricted diffusion, referred to as neurite density (ND), and increases in isotropic free water (IF) in individuals with mild cognitive impairment (MCI) and mild AD (Reas et al., 2017). These RSI measures more closely corresponded with amyloid-β than did conventional DTI metrics. Despite this sensitivity of RSI to prodromal AD, it has yet to be determined whether these measures hold value for predicting subsequent cognitive decline, and for monitoring disease progression.

Because ND is an aggregate measure of restricted diffusion, reduced ND in AD may reflect any number of cellular changes, including lower neurite count or density, axon demyelination, or cell shrinkage. ND comprises three restricted components, including diffusion in restricted isotropic (RI), restricted oriented (RO) and CF compartments, each of which may be uniquely affected by changes in cellular architecture or organization. Identifying associations of these distinct subcomponents with disease state or cognitive function may further clarify the cellular properties of neurodegenerative changes in the early stages of AD.

In this longitudinal study of healthy and mildly cognitively impaired older individuals followed clinically for approximately two years, we build upon our cross-sectional findings (Reas et al., 2017) to evaluate whether baseline RSI measures of brain microstructure predict cognitive change and whether change in microstructure over time correlates with change in cognitive function. We also more thoroughly characterize the nature of cytoarchitectural changes in aging and early AD, by examining individual components of ND (RI, RO and CF), and IF. Finally, we examine how microstructural changes are associated with normal cognitive aging among individuals without evidence of cognitive impairment.

2. Methods

2.1. Participants

Participants were recruited from the University of California, San Diego (UCSD) Shiley-Marcos Alzheimer's Disease Research Center (ADRC) and from the community. Participants underwent standardized

clinical evaluation through the ADRC Clinical Core, reviewed by two senior neurologists to provide a consensus diagnosis. Diagnosis of amnestic or multi-domain MCI and AD were based on criteria outlined by Petersen et al. (Petersen et al., 1999) and NINCDS-ADRDA clinical criteria (McKhann et al., 1984), respectively. Exclusion criteria included a Mini Mental State Exam (MMSE) score below 16, safety contraindications for MRI, uncorrected vision or hearing loss, significant illness, substance abuse, or major psychiatric or neurologic illness. Healthy controls (HC) were additionally excluded if they were taking psychotropic or cognitive enhancing medications, or demonstrated impairment on Mattis Dementia Rating Scale (DRS) or Clinical Dementia Rating tests.

From 2013 to 2016, fifty individuals, including 30 HC, 12 MCI, and eight mild AD, underwent clinical evaluation, cognitive assessment and MRI (Reas et al., 2017). From 2016 to 2017, approximately two years after baseline, participants were asked to return for follow-up clinical evaluation, cognitive assessment and MRI. Between baseline and follow-up, two HC converted to MCI, two MCI converted to AD, and one MCI participant's diagnosis was revised to HC based on improvement of neuropsychological test performance to normal; thus, 29 HC, 11 MCI and ten mild AD participated at follow-up. Henceforth, all participants are classified according to their diagnostic status at follow-up. Forty-seven participants, including 27 HC, ten MCI and ten AD, completed at least some follow-up cognitive assessment. Forty participants, including 26 HC, 10 MCI, and four AD, completed follow-up MRI. Compared to AD participants who completed follow-up MRI, those who did not return had lower mean MMSE (24.8 versus 25.8) and DRS (120 versus 127) scores at baseline. Data from one MCI and one AD patient were excluded from analysis due to poor image quality, leaving 26 HC, nine MCI and three mild AD at follow-up. Of participants who completed the second MRI scan, two HC and one MCI did not complete follow-up cognitive testing.

Because AD participants were mildly impaired and analysis of baseline data showed no differences in RSI measures between MCI and AD groups, individuals with MCI and AD were combined into an impaired group for analysis, yielding 29 HC and 21 impaired participants at baseline. Of these, 27 HC and 20 impaired participants had cognitive follow-up, and 26 HC and 12 impaired participants had MRI follow-up.

Study procedures were approved by the UCSD institutional review board and participants provided informed, written consent prior to participation. Surrogate consent was provided for participants who lacked capacity to provide meaningful consent.

2.2. Neuropsychological assessment

At baseline and follow-up, a neuropsychological test battery (Salmon and Butters, 1992) was administered by a trained examiner in a quiet room. Measures were selected for analysis based on their sensitivity to functional and cognitive impairments in AD. The MMSE, a measure of global cognition, assesses orientation, attention, language and memory (Tombaugh and McIntyre, 1992). The DRS assesses the nature and severity of dementia (Mattis, 1988). Trails B evaluates psychomotor processing speed and executive function, requiring participants to connect a sequence of alternating letters and numbers in ascending order (Reitan, 1958). Animal naming, a test of verbal semantic fluency, requires participants to name as many unique animals as possible within 60 s (Borkowsk et al., 1967; Borkowski et al., 1967). The WMS-R Logical Memory subtest requires participants to report details of a passage, immediately and after delay (Wechsler, 1987). The California Verbal Learning Test (CVLT) assesses the number of correctly recalled items from a list of 16 categorized words; immediate and delayed free recall were analyzed (Delis et al., 1987). The Consortium to Establish a Registry for Alzheimer's Disease (CERAD) delayed recall test evaluates delayed recall of a 10-item word list (Morris et al., 1989).

2.3. Imaging data acquisition

MRI data were acquired at the UCSD Center for Functional MRI on a 3.0 Tesla Discovery 750 scanner (GE Healthcare, Milwaukee, WI) with an eight-channel phased array head coil. The imaging protocol, described previously (Reas et al., 2017), was identical at baseline and follow-up and included a three-plane localizer, a sagittal 3D fast spoiled gradient echo T_1-weighted volume optimized for maximum gray/white matter contrast (TE = 3.2 ms, TR = 8.1 ms, inversion time = 600 ms, flip angle = 8°, FOV = 24 cm, frequency = 256, phase = 192, voxel size = $1 \times 1 \times 1.2$ mm, scan time 8:27), and an axial 2D single-shot pulsed-field gradient spin-echo echo-planar imaging sequence (45-directions, b-values = 0, 500, 1500, 4000 s/mm2 and 1, 6, 6, 15 unique gradient directions for each b-value, respectively; TE = 80.6 ms, TR = 8 s, frequency = 96, phase = 96, voxel size = $1.875 \times 1.875 \times 2.5$ mm, scan time 6:34).

Data processing used an automated FreeSurfer-based processing stream (http://surfer.nmr.mgh.harvard.edu) combined with tools developed at the UCSD Center for Multimodal Imaging and Genetics. RSI data were corrected for motion and eddy current distortions (J. Zhuang et al., 2006), spatial and intensity distortions (Holland et al., 2010), and distortions caused by gradient nonlinearities (Jovicich et al., 2006). Images were automatically registered to T_1-weighted structural images and rigidly re-sampled into standard orientation (Wells et al., 1996). White matter tracts were identified using AtlasTrack (Hagler et al., 2009), a probabilistic atlas that integrates fiber tract location and orientation information to estimate the a posteriori probability that a voxel belongs to a tract of interest. Partial volume effects were minimized by excluding voxels containing primarily gray matter or cerebrospinal fluid (CSF) from white matter tracts (Fischl et al., 2002). To correct for cortical surface partial volume effects, each voxel was assigned a volume fraction (0–1) according to its proportion of gray or white matter, and a weighting factor was computed using Tukey's bisquare weight function (Beaton and Tukey, 1974); volume fractions < 0.5 were weighted 0 and those > 0.5 were assigned a weight between 0 and 1, to generate gray and white matter volume fraction maps. Gray matter, white matter and CSF boundaries were automatically delineated and cortical regions of interest were identified according the Desikan-Killiany atlas (Desikan et al., 2006). All raw and processed images were visually inspected for quality. In isolated cases in which the automated surface reconstruction failed, typically due to excess motion or severe atrophy, cortical surface boundaries were manually edited by an experienced reviewer. Data were excluded from analysis if they contained motion or other artifacts, or uncorrectable mislabeling of ROIs.

2.4. Data analysis

To minimize the number of comparisons, fiber tracts of interest were selected that connect to the temporal lobe and have previously demonstrated altered diffusion signal in MCI or AD (Kitamura et al., 2013; Liu et al., 2011; Sexton et al., 2011). Tracts of interest included the fornix, hippocampal cingulum, uncinate fasciculus, inferior longitudinal fasciculus (ILF), inferior fronto-occipital fasciculus (IFO), and arcuate fasciculus. In addition, the hippocampus and entorhinal cortex were examined because of their susceptibility to early degenerative changes in AD. RI, RO and CF were measured in all fiber tracts, the hippocampus and entorhinal cortex white matter, and IF was measured in hippocampal and entorhinal cortex gray matter. IF includes contributions from CSF and excludes hindered and restricted diffusion components. RI (restricted isotropic diffusion), RO (oriented diffusion that is highly restricted perpendicular to the direction of diffusion and is not attenuated by CF), and CF (a measure of restricted diffusion in multiple directions), are respectively calculated as the square root sum of squared coefficients of the 0th, 2nd and 4th order spherical harmonics of the cylindrically restricted components within a voxel. For

comparison with gray matter morphometry, hippocampal volume (corrected for intracranial volume) and cortical thickness in the entorhinal, inferior parietal, isthmus cingulate, lateral orbitofrontal, precuneus, posterior cingulate, and parahippocampal cortices were also computed. Atrophy in these regions appears in early AD and corresponds with disease progression (McDonald et al., 2009; Risacher et al., 2009).

Continuous demographic variables were compared between HC and impaired participants using independent samples *t*-tests; sex was compared with a chi-squared test. Annualized change for cognitive test scores and RSI measures were calculated as ([follow-up – baseline] / time between tests). To exclude unreliable tests scores (due to fatigue, inattention, etc.), cognitive change scores greater than two standard deviations above the control mean were excluded from analysis. This excluded 2% of scores across all tests (seven HC scores and one AD score). Follow-up scores and cognitive change scores for cognitive function and RSI measures were compared between groups using univariate general linear modeling. To evaluate potential sex differences, initial general linear models included age and education as covariates and an interaction term between diagnostic group and sex. Because no significant sex interactions were observed, the interaction term was removed, and final models were adjusted for sex. Cognitive change scores were adjusted for baseline score. Because baseline RSI measures were not significant when included in models, analyses of RSI change did not adjust for baseline.

Partial correlations, adjusted for age, sex, education, and baseline cognitive test score, were calculated between baseline RSI measures and cognitive change scores to assess whether baseline brain microstructure predicts cognitive decline, and between RSI change scores and cognitive change scores, to assess whether microstructural change correlates with cognitive decline. Correlations were repeated between cognitive change scores and morphometric variables. When multiple RSI variables (baseline or change scores) significantly correlated with a cognitive change score, these variables were input as candidate variables in stepwise linear regressions to predict cognitive change (adjusted for age, sex, education, and baseline cognitive test score). To assess the contribution from gray matter atrophy, regressions for which RSI metrics correlated with cognitive change were repeated including candidate morphometric predictors showing significant correlations with cognitive change. To examine associations between brain microstructure and cognitive change in normal aging, partial correlations and regressions were repeated as described above, limited to HC.

Significance was set to $p < .05$ for demographic and cognitive variables, and $p < .00625$ (Bonferroni corrected for multiple comparisons across eight regions) for imaging measures. Data were analyzed using SPSS version 24.0 (IBM Corp, Armonk, NY).

3. Results

3.1. Participant characteristics

Demographics and follow-up cognitive test scores are presented for HC and impaired groups in Table 1. Impaired participants did not differ from HC by age, education, or length of cognitive or MRI follow-up ($ps > 0.05$), but the impaired group contained a greater proportion of men ($x^2 = 7.96$, $p = .005$). Compared to HC, impaired participants performed worse on all cognitive tests ($ps < 0.001$), and declined more rapidly on Trails B ($F_{(1,37)} = 6.47$, $p = .02$), logical memory immediate ($F_{(1,36)} = 8.66$, $p = .006$) and delayed ($F_{(1,35)} = 4.46$, $p = .04$) recall, and CERAD delayed recall ($F_{(1,40)} = 16.63$, $p < .001$). Impaired participants demonstrated significant decline on the MMSE, DRS, Trails B, logical memory immediate and delayed recall, and CERAD delayed recall, whereas HC demonstrated significant decline only on the DRS (annualized change score different from zero, $ps < 0.05$).

Table 1
Participant characteristics and follow-up cognitive test scores (adjusted for age, sex and education).

	HC (N = 29)	Impaired (N = 21)	Group effect
Baseline age	75.4 ± 5.2	77.5 ± 9.0	$t(48) = 0.96, p = .35$
[Range]	65–85	63–93	
Sex (% women)	69	29	$x^2 = 7.96, p = .005$
Education (years)	15.9 ± 2.5	17.2 ± 2.3	$t(48) = 1.88, p = .07$
[Range]	8–20	12–20	
Cognitive follow-up (years)	2.3 ± 0.6	2.1 ± 0.6	$t(48) = 0.65, p = .52$
[Range]	1.0–3.7	0.8–3.7	
MRI follow-up (years)	2.1 ± 0.7	2.0 ± 0.6	$t(48) = 0.66, p = .51$
[Range]	1.4–3.8	1.6–3.4	
MMSE	28.8 ± 0.9	24.4 ± 4.5	$F(1,43) = 19.69, p < .001$
DRS	139 ± 4	122 ± 15	$F(1,43) = 25.05, p < .001$
Trails B $_*$	91 ± 53	179 ± 96	$F(1,39) = 19.08, p < .001$
Verbal fluency	22.1 ± 5.8	13.1 ± 5.4	$F(1,42) = 24.59, p < .001$
Logical memory immediate recall	13.0 ± 3.3	5.7 ± 2.9	$F(1,38) = 46.96, p < .001$
Logical memory delayed recall	11.8 ± 3.7	2.8 ± 2.8	$F(1,38) = 61.30, p < .001$
CVLT immediate recall	9.5 ± 3.9	1.9 ± 2.1	$F(1,32) = 37.67, p < .001$
CVLT delayed recall	9.9 ± 3.7	1.4 ± 2.5	$F(1,32) = 48.29, p < .001$
CERAD delayed recall	6.9 ± 1.7	1.5 ± 1.8	$F(1,40) = 83.92, p < .001$

Mean ± S.D. unless otherwise noted.

 * Lower scores indicate better performance.

3.2. Differences in brain microstructure between HC and impaired individuals

Group differences in RSI metrics at follow-up (N = 38) are presented in Fig. 1. Relative to HC, impaired participants demonstrated increased IF in the hippocampus ($F(1,33) = 14.19, p < .001$) and entorhinal cortex ($F(1,33) = 8.78, p = .006$). RI was lower for impaired participants in the hippocampus ($F(1,33) = 16.74, p < .001$) and entorhinal cortex white matter ($F(1,33) = 10.15, p = .003$). CF was reduced for impaired participants in the hippocampal cingulum ($F(1,33) = 8.57, p = .006$) and hippocampus ($F(1,33) = 9.55, p = .004$).

Annualized RSI change scores for HC and impaired participants are shown in Fig. 2. RI declined significantly for impaired participants in the fornix, hippocampal cingulum, uncinate, ILF, IFO and hippocampus, and for HC in the hippocampal cingulum and IFO. Significant decline in RO was present for both groups in the IFO, and for HC in the arcuate. CF declined significantly for both groups in the ILF, IFO, and arcuate, and for HC in the uncinate. (Annualized change score different from zero, all ps < 0.006.) IF did not change significantly for either HC or impaired participants. Rates of decline differed between HC and impaired participants for hippocampal RI only, with impaired participants declining more rapidly ($F(1,33) = 11.98, p = .002$).

3.3. Brain microstructure and cognitive decline

Baseline RSI measures (N = 47) and RSI change scores (N = 35) significantly correlated with cognitive change scores are presented in Table 2A. Associations of baseline RSI or change variables with cognitive change scores are presented in Fig. 3. Hippocampal RI and entorhinal IF correlated with verbal fluency change; when these variables were input into stepwise linear regressions, only lower baseline hippocampal RI independently predicted greater verbal fluency decline (standardized β = 0.58, R^2 change = 0.20, p = .001, full model adjusted R^2 = 0.24; adjusted for age, sex, education, baseline verbal fluency score). When both morphometric and RSI measures were included as predictors, lower baseline hippocampal volume (standardized β = 0.45, R^2 change = 0.23, p = .006) and isthmus cingulate thickness (standardized β = 0.39, R^2 change = 0.10, p = .006) predicted greater verbal fluency decline (full model adjusted R^2 = 0.37).

Decline in hippocampal RI was associated with decline on the DRS (partial r = 0.49, p = .006; adjusted for age, sex, education, baseline DRS score). Change in entorhinal, hippocampal and ILF RI, and change in entorhinal IF were correlated with Trails B change; when these variables were input into stepwise linear regressions only reduced entorhinal RI was independently associated with decline on the Trails B (standardized β = −0.62, R^2 change = 0.33, p < .001, full model adjusted R^2 = 0.43; adjusted for age, sex, education, baseline Trails B score). Change in gray matter morphometry was not correlated with rates of change on these tests.

3.4. Brain microstructure and cognitive decline in HC

Baseline RSI (N = 27) and RSI change (N = 24) variables that significantly correlated with cognitive change scores for HC are presented in Table 2B. Associations of baseline RSI measures or RSI change scores with cognitive change for HC are presented in Fig. 4. Within HC, higher baseline hippocampal cingulum RO predicted more rapid logical memory immediate recall decline (partial r = −0.71, p < .001), and higher baseline ILF CF predicted more rapid logical memory delayed recall decline (partial r = −0.62, p = .002). Greater decline in fornix RO was associated with faster CERAD delayed recall decline (partial r = 0.62, p = .004). Baseline gray matter morphometry did not predict memory change, and change in gray matter did not correlate with change in memory.

4. Discussion

RSI measures of gray and white matter microarchitecture were associated with cognitive decline, and changed more rapidly over a two-year follow-up period in individuals with MCI and mild AD than in cognitively healthy older adults. Baseline levels and rates of change in mean restricted diffusion in the medial temporal lobe correlated with rates of cognitive decline and progression of dementia severity. Distinct microstructural changes were present in older adults without cognitive impairment. In healthy controls, baseline orientated diffusion and structural complexity in white matter association fibers predicted memory decline, and change in orientated diffusion over time correlated with memory decline.

Follow-up cross-sectional data described here validate previously reported baseline data in this cohort, with reduced ND and higher IF for cognitively impaired participants, and strong group differences observed in the hippocampus and entorhinal cortex (Reas et al., 2017). We expand upon these findings to reveal that reduced ND is largely driven by lower mean restricted diffusion and loss of structural complexity (CF). We further report that hippocampal restricted isotropic diffusion predicts cognitive decline, and that rates of change in
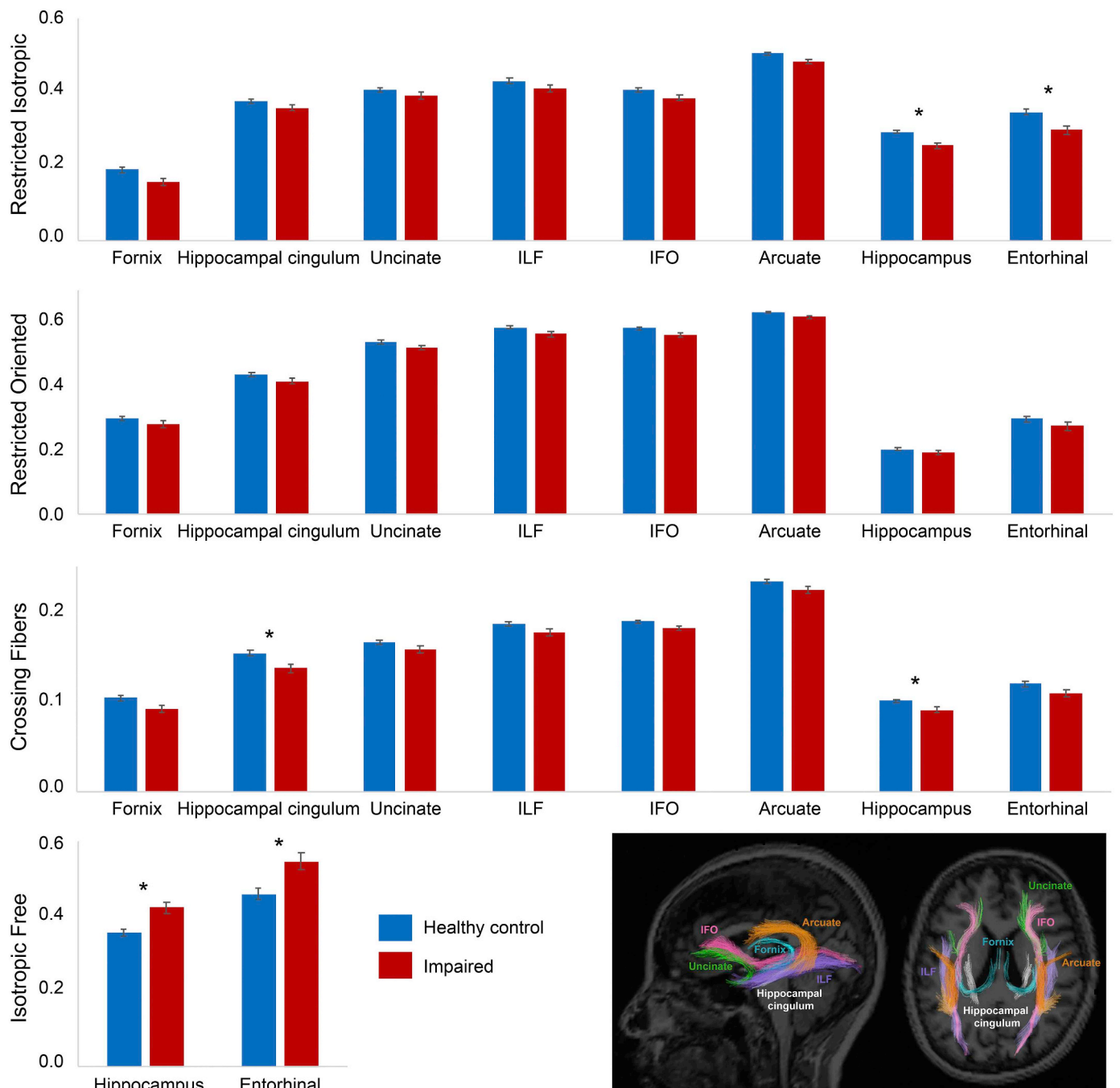
Fig. 1. Mean (± S.E.) RSI measures (adjusted for age, sex, and education) at follow-up for HC ($N = 26$) and impaired ($N = 12$) participants. Tracts of interest are labeled for an example HC. * Significant group difference, $p < .00625$.

hippocampal and entorhinal restricted isotropic diffusion correlate with cognitive decline, supporting the value of RSI for predicting and monitoring disease progression.

DTI studies have similarly reported that altered medial temporal lobe microstructure predicts memory decline (Lancaster et al., 2016; L. Zhuang et al., 2012), is sensitive to MCI and correlates with cognitive function (Fellgiebel et al., 2004; Hong et al., 2013; Kantarci et al., 2001). Our findings add to this literature by localizing the strongest associations between altered microstructure and cognitive decline to the hippocampus and entorhinal cortex. The hippocampus is critically involved in encoding new memories and is an early target of neuropathology and atrophy in AD. The entorhinal cortex is a critical hub of AD pathogenesis and demonstrates the earliest neuropathological

events in AD, including the appearance of tau tangles, synapse loss and cell death (Braak and Braak, 1991; Gomez-Isla et al., 1996; Hyman et al., 1984; Scheff et al., 2006). The observation that fine architectural changes in the hippocampus and entorhinal cortex in prodromal AD correspond with clinical and cognitive progression is in line with their role at the center of an early pathological cascade.

Because of its ability to measure tissue diffusion at different size scales and with higher order representations of orientation, RSI provides additional information regarding cytoarchitectural properties, and thus affords more comprehensive characterization than DTI of the microstructural brain changes that manifest in prodromal AD. This investigation builds upon the DTI literature to identify reduced restricted diffusion as the strongest factor underlying medial temporal lobe
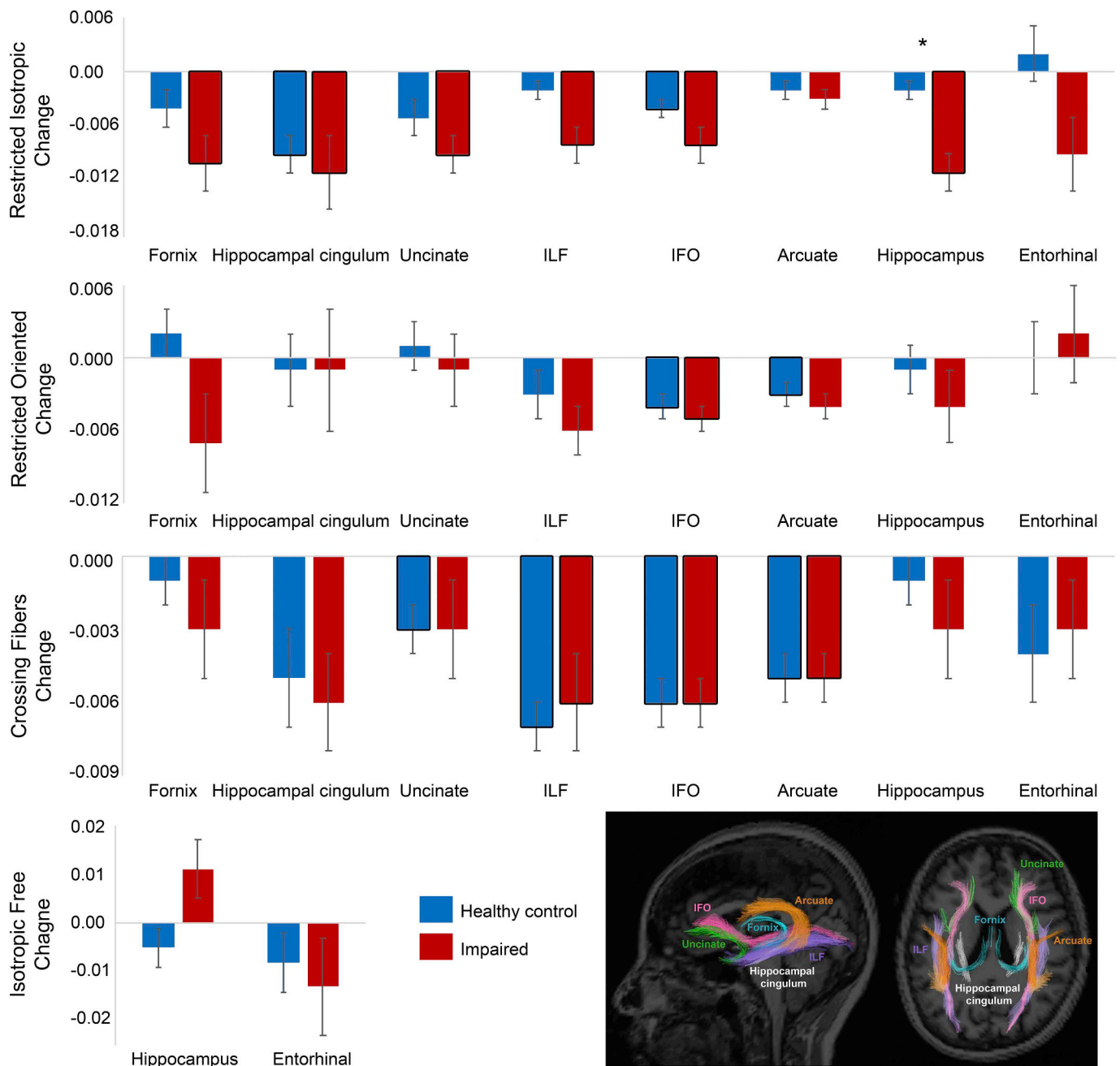
Fig. 2. Annualized RSI change scores (± S.E.) (adjusted for age, sex, and education) for HC (*N* = 26) and impaired (*N* = 12) participants. Tracts of interest are labeled for an example HC. * Significant group difference, *p* < .00625. Significant change (i.e., significant difference from zero, *p* < .00625) is indicated by outlined bars.

changes in diffusion signal in prodromal AD. It further expands upon our prior findings of reduced white matter ND in MCI and AD (Reas et al., 2017) to tease apart the cellular contributions to reduced ND, and to identify their relationship to cognitive decline. Cognitive impairment and decline most strongly associated with reduced RI, a measure of mean restricted diffusion. Declining RI may reflect morphological changes in neurites or neuronal or glial cell bodies, such as shrinkage or dystrophy. Dystrophic neurons early in AD may underlie circuit dysfunction that impairs synaptic signaling (Grace et al., 2002), and dystrophic microglia colocalize with tau pathology in early AD (Streit et al., 2009). Accounting for cortical atrophy attenuated the association between hippocampal RI and verbal fluency decline, supporting the interpretation that the effect of lower hippocampal RI on verbal fluency decline may be partially driven by volume loss. However, the

associations of cognitive decline with declining hippocampal and entorhinal RI were independent of morphometric change, indicating that medial temporal microstructure provides information beyond that of cortical atrophy. In addition, CF in the hippocampus and hippocampal cingulum were reduced in impaired individuals. Reduced CF may reflect loss of structural complexity with lower dendritic or axonal count or density, or neurite reorganization.

Distinct microstructural changes were associated with cognitive decline in older individuals without evidence of cognitive impairment. In cognitively normal individuals, only white matter changes correlated with memory decline, and gray matter morphometry did not improve prediction of cognitive decline beyond prediction by white matter microstructure. RO and CF related to cognitive decline in HC, in contrast to the full sample, which demonstrated no associations between these

Table 2
RSI measures (baseline or change scores) significantly correlated with annualized cognitive change scores (adjusted for age, sex, education, and baseline cognitive test score), for all participants (A) and healthy controls (B).

| Test	RSI measure	Correlation
A. All participants		
Verbal fluency change	Baseline Hippocampus RI	$r = 0.48$, $p = .001$
	Baseline Entorhinal IF	$r = -0.43$, $p = .004$
DRS change	Hippocampus RI change	$r = 0.49$, $p = .006$
Trails B change	Entorhinal RI change	$r = -0.64$, $p < .001$
	Hippocampus RI change	$r = -0.55$, $p = .002$
	Entorhinal IF change	$r = 0.51$, $p = .004$
	ILF RI change	$r = -0.49$, $p = .006$
B. Healthy controls		
Logical memory immediate recall change	Baseline Hippocampal Cingulum RO	$r = -0.71$, $p < .001$
Logical memory delayed recall change	Baseline ILF CF	$r = -0.62$, $p = .002$
CERAD delayed recall change	Fornix RO change	$r = 0.62$, $p = .004$

measures and cognitive change. Decline in white matter RO, an estimate of oriented intracellular diffusion, may result from demyelination, or reduced axon count or density. Here, declining RO in the fornix correlated with episodic memory decline. Others have reported that altered fornix microstructure is an early predictor of cognitive decline

and biomarker of preclinical AD and progressive MCI (Douaud et al., 2013; Fletcher et al., 2013; L. Zhuang et al., 2012; L. Zhuang et al., 2013). Unexpectedly, increased hippocampal cingulum RO and greater structural complexity in the ILF predicted logical memory decline. Trends ($p < .06$) for correlations between higher baseline cortical thickness and logical memory decline in HC indicate that the observed negative correlations are unlikely to be artifacts of the RSI metrics. Though correlations between white matter integrity and cognitive performance in older age have been reported, longitudinal studies on associations between brain microstructure and cognitive decline in normal aging are sparse and inconclusive. Whether regional increases in the integrity and complexity of association fibers reflect compensatory white matter reorganization in response to normal brain aging (Craik and Rose, 2012), or signal aberrant neural changes that directly contribute to memory deficits, warrants further investigation.

Limitations of this study include unequal proportions of men and women in the HC and impaired groups. Thus, despite adjusting our analyses for sex, it is possible that some observed group differences may have arisen from sex differences in brain microstructure. Although we did not find interactions by sex, we did not have sufficient power to detect sex differences in these metrics. Given the mounting evidence for sex differences in risk factors, pathogenesis and biomarkers of AD (Ferretti et al., 2018), additional study in adequately powered samples will be critical to determine whether sex differences exist in the associations between brain microstructure and cognitive symptoms. In addition, we were limited by loss of participants to follow-up, which reduced statistical power and prevented us from comparing MCI to mild AD, or examining associations between RSI metrics and cognitive function within impaired individuals. Too few participants clinically
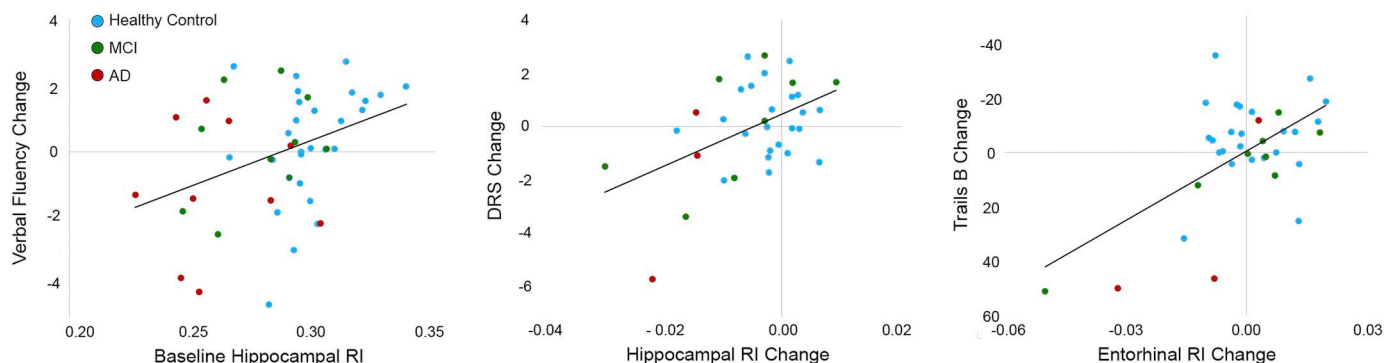
Fig. 3. Significant associations between baseline RSI measures (HC, $N = 27$; impaired, $N = 20$) or annualized RSI scores (HC, $N = 24$; impaired, $N = 11$) and annualized cognitive change (adjusted for age, sex, education, and baseline cognitive test score). The y-axis for Trails B change is inverted because positive change indicates declining performance.
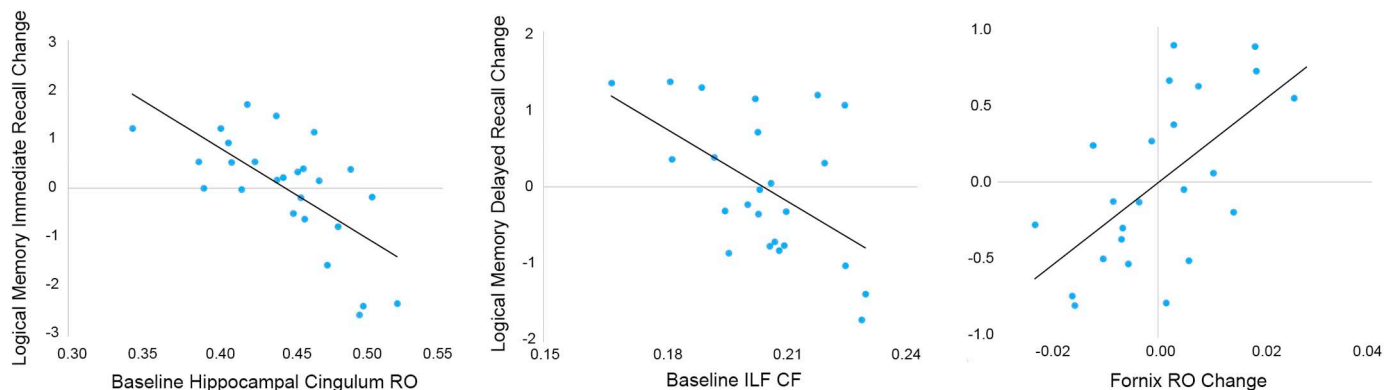
Fig. 4. Significant associations between baseline RSI measures ($N = 27$) or annualized RSI scores ($N = 24$) and annualized cognitive change (adjusted for age, sex, education, and baseline cognitive test score) for healthy controls.

converted over the course of follow-up to assess the efficacy of RSI metrics as preclinical indictors. However, even in the absence of overt clinical conversion, brain microstructure predicted subsequent cognitive decline, suggesting that RSI metrics are sensitive to even subtle brain changes in mild disease stages. Further investigation in a larger cohort will clarify the value of RSI in identifying markers of incipient AD in presymptomatic individuals.

In summary, we report that changes in medial temporal lobe gray and white matter microstructure, including increased free diffusion, reduced restricted diffusion and reduced structural complexity, were associated with prodromal and mild AD. These alterations predicted cognitive decline, and magnitude of microstructural change over time correlated with rate of cognitive decline. Distinct changes in white matter microstructure correlated with memory decline in cognitively normal older individuals. These findings help to better characterize the microstructural brain changes occurring during the early stages of AD progression and may inform about key neurophysiological changes precipitating dementia.

Acknowledgments

Conflicts of interest

LKM holds stock in CorTechs Laboratories, Inc. JBB has served on advisory boards for Elan, Bristol-Myers Squibb, Avanir, Novartis, Genentech, and Eli Lilly and holds stock in CorTechs Labs, Inc. and Human Longevity, Inc. AMD is a founder and holds equity in CorTechs Laboratories, Inc., and serves on its Scientific Advisory Board. He is a member of the Scientific Advisory Board of Human Longevity, Inc. and receives funding through research agreements with General Electric Healthcare and Medtronic, Inc. This arrangement have been reviewed and approved by UCSD, in accordance with its conflict of interest policies. NSW is Chief Technology Officer and holds equity in Healthlytics, Inc. DG has served on the advisory board for vTv Pharmaceuticals and Data Monitoring Boards for Proclara and Cognition Therapeutics. No other authors declare competing financial interests.

References

Agosta, F., Pievani, M., Sala, S., Geroldi, C., Galluzzi, S., Frisoni, G.B., Filippi, M., 2011. White matter damage in Alzheimer disease and its relationship to gray matter atrophy. Radiology 258 (3), 853–863 (doi:radiol.10101284 [pii] 21148/radiol.10101284).

Amlien, I.K., Fjell, A.M., 2014. Diffusion tensor imaging of white matter degeneration in Alzheimer's disease and mild cognitive impairment. Neuroscience 276, 206–215. https://doi.org/10.1016/j.neuroscience.2014.02.017.

Beaton, A.E., Tukey, J.W., 1974. The fitting of power series, meaning polynomials, illustrated on band-spectroscopic data. Technometrics 16 (2), 147–185.

Borkowski, J.G., Benton, A.L., Spreen, O., 1967. Word Fluency and Brain damage. Neuropsychologia 5 (2). https://doi.org/10.1016/0028-3932(67)90015-2.

Borkowski, J.G., Benton, A.L., Spreen, O., 1967. Word fluency and brain damage. Neuropsychologia 5 (2), 135–140.

Braak, H., Braak, E., 1991. Neuropathological stageing of Alzheimer-related changes. Acta Neuropathol. 82 (4), 239–259.

Brueggen, K., Dyrba, M., Barkhof, F., Hausner, L., Filippi, M., Nestor, P.J., Teipel, S.J., 2015. Basal forebrain and hippocampus as predictors of conversion to Alzheimer's disease in patients with Mild Cognitive Impairment - a multicenter DTI and volumetry study. J. Alzheimers Dis. 48 (1), 197–204. https://doi.org/10.3233/JAD-150063.

Craik, F.I., Rose, N.S., 2012. Memory encoding and aging: a neurocognitive perspective. Neurosci. Biobehav. Rev. 36 (7), 1729–1739. https://doi.org/10.1016/j.neubiorev.2011.11.007.

Delis, D.C., Kramer, J.H., Kaplan, E., Thompkins, B.A.O., 1987. CVLT, California Verbal Learning Test: Adult Version: Manual: Psychological Corporation.

Desikan, R.S., Segonne, F., Fischl, B., Quinn, B.T., Dickerson, B.C., Blacker, D., Killiany, R.J., 2006. An automated labeling system for subdividing the human cerebral cortex

on MRI scans into gyral based regions of interest. NeuroImage 31 (3), 968–980. https://doi.org/10.1016/j.neuroimage.2006.01.021.

Douaud, G., Menke, R.A., Gass, A., Monsch, A.U., Rao, A., Whitcher, B., Smith, S., 2013. Brain microstructure reveals early abnormalities more than two years prior to clinical progression from mild cognitive impairment to Alzheimer's disease. J. Neurosci. 33 (5), 2147–2155. https://doi.org/10.1523/JNEUROSCI.4437-12.2013.

Du, A.T., Schuff, N., Amend, D., Laakso, M.P., Hsu, Y.Y., Jagust, W.J., Weiner, M.W., 2001. Magnetic resonance imaging of the entorhinal cortex and hippocampus in mild cognitive impairment and Alzheimer's disease. J. Neurol. Neurosurg. Psychiatry 71 (4), 441–447.

Fellgiebel, A., Wille, P., Muller, M.J., Winterer, G., Scheurich, A., Vucurevic, G., Stoeter, P., 2004. Ultrastructural hippocampal and white matter alterations in mild cognitive impairment: a diffusion tensor imaging study. Dement. Geriatr. Cogn. Disord. 18 (1), 101–108. https://doi.org/10.1159/000077817.

Ferretti, M.T., Iulita, M.F., Cavedo, E., Chiesa, P.A., Schumacher Dimech, A., Santuccione Chadha, A., the Alzheimer Precision Medicine, I, 2018. Sex differences in Alzheimer disease - the gateway to precision medicine. Nat. Rev. Neurol. https://doi.org/10.1038/s41582-018-0032-9.

Fischl, B., Salat, D.H., Busa, E., Albert, M., Dieterich, M., Haselgrove, C., Dale, A.M., 2002. Whole brain segmentation: automated labeling of neuroanatomical structures in the human brain. Neuron 33 (3), 341–355.

Fletcher, E., Raman, M., Huebner, P., Liu, A., Mungas, D., Carmichael, O., Decarli, C., 2013. Loss of fornix white matter volume as a predictor of cognitive impairment in cognitively normal elderly individuals. JAMA Neurol 70 (11), 1389–1395 (doi:1735198 pii, 181001/jamaneurol.2013.3263).

Gomez-Isla, T., Price, J.L., McKeel Jr., D.W., Morris, J.C., Growdon, J.H., Hyman, B.T., 1996. Profound loss of layer II entorhinal cortex neurons occurs in very mild Alzheimer's disease. J. Neurosci. 16 (14), 4491–4500.

Grace, E.A., Rabiner, C.A., Busciglio, J., 2002. Characterization of neuronal dystrophy induced by fibrillar amyloid beta: implications for Alzheimer's disease. Neuroscience 114 (1), 265–273.

Hagler Jr., D.J., Ahmadi, M.E., Kuperman, J., Holland, D., McDonald, C.R., Halgren, E., Dale, A.M., 2009. Automated white-matter tractography using a probabilistic diffusion tensor atlas: Application to temporal lobe epilepsy. Hum. Brain Mapp. 30 (5), 1535–1547. https://doi.org/10.1002/hbm.20619.

Holland, D., Kuperman, J.M., Dale, A.M., 2010. Efficient correction of inhomogeneous static magnetic field-induced distortion in Echo Planar Imaging. NeuroImage 50 (1), 175–183. https://doi.org/10.1016/j.neuroimage.2009.11.044.

Hong, Y.J., Yoon, B., Lim, S.C., Shim, Y.S., Kim, J.Y., Ahn, K.J., Yang, D.W., 2013. Microstructural changes in the hippocampus and posterior cingulate in mild cognitive impairment and Alzheimer's disease: a diffusion tensor imaging study. Neurol. Sci. 34 (7), 1215–1221. https://doi.org/10.1007/s10072-012-1225-4.

Hyman, B.T., Van Hoesen, G.W., Damasio, A.R., Barnes, C.L., 1984. Alzheimer's disease: cell-specific pathology isolates the hippocampal formation. Science 225 (4667), 1168–1170.

Jack Jr., C.R., Petersen, R.C., Xu, Y., O'Brien, P.C., Smith, G.E., Ivnik, R.J., Kokmen, E., 2000. Rates of hippocampal atrophy correlate with change in clinical status in aging and AD. Neurology 55 (4), 484–489.

Jovicich, J., Czanner, S., Greve, D., Haley, E., van der Kouwe, A., Gollub, R., Dale, A., 2006. Reliability in multi-site structural MRI studies: effects of gradient non-linearity correction on phantom and human data. NeuroImage 30 (2), 436–443. https://doi.org/10.1016/j.neuroimage.2005.09.046.

Kantarci, K., Jack Jr., C.R., Xu, Y.C., Campeau, N.G., O'Brien, P.C., Smith, G.E., Petersen, R.C., 2001. Mild cognitive impairment and Alzheimer disease: regional diffusivity of water. Radiology 219 (1), 101–107. https://doi.org/10.1148/radiology.219.1.r01ap14101.

Kantarci, K., Murray, M.E., Schwarz, C.G., Reid, R.I., Przybelski, S.A., Lesnick, T., Dickson, D.W., 2017. White-matter integrity on DTI and the pathologic staging of Alzheimer's disease. Neurobiol. Aging 56, 172–179. https://doi.org/10.1016/j.neurobiolaging.2017.04.024.

Kitamura, S., Kiuchi, K., Taoka, T., Hashimoto, K., Ueda, S., Yasuno, F., Kishimoto, T., 2013. Longitudinal white matter changes in Alzheimer's disease: a tractography-based analysis study. Brain Res. 1515, 12–18. https://doi.org/10.1016/j.brainres.2013.03.052.

Lancaster, M.A., Seidenberg, M., Smith, J.C., Nielson, K.A., Woodard, J.L., Durgerian, S., Rao, S.M., 2016. Diffusion Tensor Imaging Predictors of Episodic memory Decline in healthy Elders at Genetic Risk for Alzheimer's Disease. J. Int. Neuropsychol. Soc. 22 (10), 1005–1015. https://doi.org/10.1017/S1355617716000904.

Liu, Y., Spulber, G., Lehtimaki, K.K., Kononen, M., Hallikainen, I., Grohn, H., Soininen, H., 2011. Diffusion tensor imaging and tract-based spatial statistics in Alzheimer's disease and mild cognitive impairment. Neurobiol. Aging 32 (9), 1558–1571. https://doi.org/10.1016/j.neurobiolaging.2009.10.006.

Mattis, S., 1988. *Dementia Rating Scale. Professional Manual.* Florida: Psychological Assessment Resources.

McDonald, C.R., McEvoy, L.K., Gharapetian, L., Fennema-Notestine, C., Hagler Jr., D.J., Holland, D., Alzheimer's Disease Neuroimaging, I., 2009. Regional rates of neocortical atrophy from normal aging to early Alzheimer disease. Neurology 73 (6), 457–465. https://doi.org/10.1212/WNL.0b013e3181b16431.

McDonald, C.R., Gharapetian, L., McEvoy, L.K., Fennema-Notestine, C., Hagler Jr., D.J., Holland, D., Alzheimer's Disease Neuroimaging, I., 2012. Relationship between regional atrophy rates and cognitive decline in mild cognitive impairment. Neurobiol. Aging 33 (2), 242–253. https://doi.org/10.1016/j.neurobiolaging.2010.03.015.

McEvoy, L.K., Fennema-Notestine, C., Roddey, J.C., Hagler Jr., D.J., Holland, D., Karow, D.S., Alzheimer's Disease Neuroimaging, I., 2009. Alzheimer disease: quantitative structural neuroimaging for detection and prediction of clinical and structural changes in mild cognitive impairment. Radiology 251 (1), 195–205. https://doi.org/

10.1148/radiol.2511080924.

McKhann, G., Drachman, D., Folstein, M., Katzman, R., Price, D., Stadlan, E.M., 1984. Clinical diagnosis of Alzheimer's disease: report of the NINCDS-ADRDA Work Group under the auspices of Department of Health and Human Services Task Force on Alzheimer's Disease. Neurology 34 (7), 939–944.

Mielke, M.M., Okonkwo, O.C., Oishi, K., Mori, S., Tighe, S., Miller, M.I., Lyketsos, C.G., 2012. Fornix integrity and hippocampal volume predict memory decline and progression to Alzheimer's disease. Alzheimers Dement. 8 (2), 105–113. https://doi.org/10.1016/j.jalz.2011.05.2416.

Morris, J. C., Heyman, A., Mohs, R. C., Hughes, J. P., van Belle, G., Fillenbaum, G., . . . Clark, C. (1989). The Consortium to establish a Registry for Alzheimer's Disease (CERAD). Part I. Clinical and neuropsychological assessment of Alzheimer's disease. Neurology, 39(9), 1159–1165.

Nowrangi, M.A., Lyketsos, C.G., Leoutsakos, J.M., Oishi, K., Albert, M., Mori, S., Mielke, M.M., 2013. Longitudinal, region-specific course of diffusion tensor imaging measures in mild cognitive impairment and Alzheimer's disease. Alzheimers Dement. 9 (5), 519–528. https://doi.org/10.1016/j.jalz.2012.05.2186.

Petersen, R.C., Smith, G.E., Waring, S.C., Ivnik, R.J., Tangalos, E.G., Kokmen, E., 1999. Mild cognitive impairment: clinical characterization and outcome. Arch. Neurol. 56 (3), 303–308.

Reas, E.T., Hagler Jr., D.J., White, N.S., Kuperman, J.M., Bartsch, H., Cross, K., McEvoy, L.K., 2017. Sensitivity of restriction spectrum imaging to memory and neuropathology in Alzheimer's disease. Alzheimers Res. Ther. 9 (1), 55. https://doi.org/10.1186/s13195-017-0281-7.

Reitan, R.M., 1958. Validity of the trail making test as an indicator of organic brain damage. Percept. Mot. Skills 8, 271–276.

Risacher, S.L., Saykin, A.J., West, J.D., Shen, L., Firpi, H.A., McDonald, B.C., Alzheimer's Disease Neuroimaging, I., 2009. Baseline MRI predictors of conversion from MCI to probable AD in the ADNI cohort. Curr. Alzheimer Res. 6 (4), 347–361.

Salmon, D., Butters, N., 1992. Neuropsychological assessment of dementia in the elderly. Principles of geriatric neurology. Vol. 144. FA Davis, Philadelphia, pp. 63.

Scheff, S.W., Price, D.A., Schmitt, F.A., Mufson, E.J., 2006. Hippocampal synaptic loss in early Alzheimer's disease and mild cognitive impairment. Neurobiol. Aging 27 (10), 1372–1384 (doi:S0197-4580(05)00283-6 pii461016/j.neurobiolaging.2005.09.012).

Sexton, C.E., Kalu, U.G., Filippini, N., MacKay, C.E., Ebmeier, K.P., 2011. A meta-analysis of diffusion tensor imaging in mild cognitive impairment and Alzheimer's disease. Neurobiol. Aging 32 (12), 2322 e2325–2318. https://doi.org/10.1016/j.neurobiolaging.2010.05.019.

Streit, W.J., Braak, H., Xue, Q.S., Bechmann, I., 2009. Dystrophic (senescent) rather than activated microglial cells are associated with tau pathology and likely precede neurodegeneration in Alzheimer's disease. Acta Neuropathol. 118 (4), 475–485. https://doi.org/10.1007/s00401-009-0556-6.

Tombaugh, T.N., McIntyre, N.J., 1992. The mini-mental state examination: a comprehensive review. J. Am. Geriatr. Soc. 40 (9), 922–935.

Wechsler, D., 1987. WMS-R: Wechsler memory scale-revised: Psychological Corporation.

Wells III, W.M., Viola, P., Atsumi, H., Nakajima, S., Kikinis, R., 1996. Multi-modal volume registration by maximization of mutual information. Med. Image Anal. 1 (1), 35–51.

White, N.S., Leergaard, T.B., D'Arceuil, H., Bjaalie, J.G., Dale, A.M., 2013. Probing tissue microstructure with restriction spectrum imaging: Histological and theoretical validation. Hum. Brain Mapp. 34 (2), 327–346. https://doi.org/10.1002/hbm.21454.

Zhuang, J., Hrabe, J., Kangarlu, A., Xu, D., Bansal, R., Branch, C.A., Peterson, B.S., 2006. Correction of eddy-current distortions in diffusion tensor images using the known directions and strengths of diffusion gradients. J. Magn. Reson. Imaging 24 (5), 1188–1193. https://doi.org/10.1002/jmri.20727.

Zhuang, L., Sachdev, P.S., Trollor, J.N., Kochan, N.A., Reppermund, S., Brodaty, H., Wen, W., 2012. Microstructural white matter changes in cognitively normal individuals at risk of amnestic MCI. Neurology 79 (8), 748–754 doi:WNL.0b013e3182661f4d. ([pii] 551212/WNL.0b013e3182661f4d).

Zhuang, L., Sachdev, P.S., Trollor, J.N., Reppermund, S., Kochan, N.A., Brodaty, H., Wen, W., 2013. Microstructural white matter changes, not hippocampal atrophy, detect early amnestic mild cognitive impairment. PLoS One 8 (3), e58887. https://doi.org/10.1371/journal.pone.0058887.